Cubic SiC formation on the C-face of 6H-SiC (0001) substrates

Remigijus Vasiliauskas, Sandrine Juillaguer, Mikael Syväjärvi and Risitza Yakimova

Linköping University Post Print

N.B.: When citing this work, cite the original article.

Original Publication:

Remigijus Vasiliauskas, Sandrine Juillaguer, Mikael Syväjärvi and Risitza Yakimova, Cubic SiC formation on the C-face of 6H-SiC (0001) substrates, 2012, Journal of Crystal Growth, (348), 1, 91-96.
http://dx.doi.org/10.1016/j.jcrysgro.2012.03.053
Copyright: Elsevier
http://www.elsevier.com/

Postprint available at: Linköping University Electronic Press
http://urn.kb.se/resolve?urn=urn:nbn:se:liu:diva-76363

Cubic SiC formation on the C-face of 6H-SiC (0001) substrates

Remigijus Vasiliauskas[a,*], Sandrine Juillaguet[b], Mikael Syväjärvi[a] and Rositza Yakimova[a]

[a]Department of Physics, Chemistry and Biology, Linköping University, SE-581 83 Linköping, Sweden

[b]CNRS and Université Montpellier 2, Laboratoire Charles Coulomb, cc074-GES, 34095 Montpellier cedex 5, France

Abstract. Nucleation and subsequent growth of cubic SiC (111) on Si- and C-faces of nominally on-axis 6H-SiC substrates was investigated. More uniform nuclei and twin boundary distribution was observed when 3C-SiC was grown on the C-face. This was attributed to a lower critical supersaturation ratio. A new type of defects which appear as pits in the C-face 3C-SiC layers related to homoepitaxial 6H-SiC spiral growth was found and described. The evaluation of the growth driving force for both polar faces showed that the homoepitaxial 6H-SiC spirals were not overgrown on the C-face due to low maximum supersaturation ratio. The XRD ω-rocking characterization shows a better structural quality of the 3C-SiC was grown on the Si-face, however on the C-face the uniformity over the whole sample was higher. Unintentional doping by N (~10^{16} cm^{-3}) was slightly higher on the C-face while Al doping was higher (~10^{14} cm^{-3}) on the Si-face of the grown material, similarly to the doping of hexagonal SiC polytypes.

Keywords: A1. Nucleation, A1. Characterization, A1. Polar surfaces A3. Vapor phase epitaxy, B1. Cubic Silicon Carbide.

1. Introduction

* *Corresponding author.* Tel.: +46-13-281704; fax: +46-13-137568.
E-mail address: remis@ifm.liu.se (R. Vasiliauskas)

Cubic silicon carbide (3C-SiC) is a wide bandgap semiconductor with potential advantages compared to the hexagonal SiC polytypes 4H-SiC and 6H-SiC. The 3C-SiC has the highest saturated electron velocity and isotropic physical properties due to a cubic lattice. It was shown that 3C-SiC is a suitable substrate for growth of monolayer graphene [1]. The smaller bandgap of 3C-SiC is favorable concerning the interface state density in SiO_2/3C-SiC and graphene/3C-SiC material systems. Additionally, ideal tandem solar cells produced from 3C-SiC should achieve ~60% efficiency [2].

The 3C-SiC material discussed here was grown in the (111) direction on top of on-axis 6H-SiC (0001) substrates. The lattice mismatch in this system is below 0.1% and problems with thermal mismatch are substantially reduced compared to the growth of 3C-SiC on silicon substrates. Therefore from the point of view of the general prerequisites for epitaxy, 6H-SiC appears to be a perfect substrate for growth of cubic SiC [3-6].

When cut perpendicular to the c-axis the hexagonal polytypes of SiC exhibit polar surfaces which are referred to as Si- or C-terminated surfaces or in short as Si- and C-face, respectively. The cubic polytype possesses similar polar surfaces along the [111] direction. These surfaces are characterized by having a Si (C) top layer atoms with one dangling bond and three back bonds connecting them with their three nearest neighbor C (Si) atoms on the second layer. It has been common to grow 3C-SiC on the Si-face of hexagonal SiC polytypes as the quality of the 3C-SiC material on this face is higher [7,8]. On the other hand, a substantially higher two dimensional electron gas sheet densities could be achieved if the material is grown on the C-face [9], which may be beneficial for electronic devices such as high electron mobility transistors. Nonetheless, 3C-SiC growth on C-face remains immature due to lack of systematic studies.

The Si- and C-faces have different surface free energies. Thus, different nucleation and growth of 3C-SiC should be expected. In this work we have studied the nucleation and growth on the C-face and compared it with the growth on Si-face.

2. **Experimental**

In the current work the growth of 3C-SiC layers was performed by sublimation epitaxy in a vertical quartz tube reactor [10]. The two inch nominally on-axis 6H-SiC substrates with silicon (0001) and carbon $(000\overline{1})$ faces prepared for epitaxy were cut in quarters and further used for 3C-SiC growth. The growth was performed in a graphite crucible placed in an evacuated chamber (base vacuum 10^{-5} mbar). The crucible was heated inductively with a radio-frequency (~45 kHz) coil. The growth temperature was measured on the top of the crucible using two-color pyrometer. A polycrystalline SiC source and a 6H-SiC substrate were separated with 1 mm thick graphite spacer. A temperature gradient was applied, which was the driving force for the transport of sublimed species from the source to the substrate. To avoid source graphitization, carbon getter (tantalum foil) was used.

In order to find optimal conditions for growth of 3C-SiC, growth on each face of SiC was performed by changing temperature from 1675°C to 1775°C by 50 degrees. Temperature ramp up of 5K/min and growth time of 30 min was applied for all experiments. Growth rates were 200-250 µm/h at 1725°C and 450-500 µm/h at 1775°C. No significant difference in the overall growth rate was observed between Si- and C-faces.

The 3C-SiC polytype was identified by the color (yellow for 3C-SiC and transparent/bluish for 6H-SiC) in an optical microscope with Nomarski interference contrast (OM) by using transmitted light and confirmed by Raman spectroscopy measurements. Surface morphology of the grown layers was studied with OM and Atomic Force Microscope (AFM). Low temperature photoluminescence (LTPL) spectroscopy was applied in order to estimate the type and concentration of residual impurities. The LTPL spectra were collected at 5 K, using 20 mW of the 244 nm wavelength of a frequency doubled Ar+-ion laser as excitation source. Structural characterization was performed via omega angle (rocking scans) x-ray diffraction (XRD) measurements by using the (111) Bragg reflection. A Philips X'Pert high-resolution x-ray diffraction (HRXRD) diffractometer operating in triple-axis mode with Cu Kα1 anode at 45 kV voltage and 40 mA current was used in this work. The HRXRD was operated with (Ge 220) four reflection monochromator at the tube side

and three reflection monochromator at the detector side.

3. Results and discussion

3.1 Growth of cubic SiC

The Si- and C-faces of SiC along the (0001) direction have different surface free energies. The difference in the surface free energies of these faces is due to downward relaxation of the top-layer atoms. This relaxation is caused by bond-bending angular forces at the second-layer atoms, which affect C atoms stronger than Si atoms. The larger displacement of surface atoms on the C-face gives energy gain of 0.30 eV and on the Si-face the displacement is smaller and the energy gain is only 0.09 eV [11]. As a result the surface free energy of the C-face 6H-SiC is 718 erg/cm^2 and of the Si-face is 1767 erg/cm^2 [12]. Due to similarity of three Si-C bilayer stacking of 6H-SiC along the [0001] direction and of 3C-SiC along the [111] direction, the surface free energies of these polytypes are considered similar. This information gives an idea how nucleation and growth on both faces will occur.

Although grown with a high matching degree in terms of chemical composition and lattice parameters, the 3C-SiC on 6H-SiC substrates contains a number of specific defects because of the different crystallographic geometries. Due to the twofold possibility to arrange the Si-C bilayer stacking along the c-axis on a (0001) 6H-SiC substrate, two different domains of (111) 3C-SiC may form. These are called twins. The boundaries between the twins are known as twin boundaries (TBs), which are extended defects [5]. Other common defects in cubic SiC are stacking faults (SFs) and 6H-SiC inclusions. The latter ones form due to local fluctuations of the supersaturation ratio on the growth surface [13]. The disturbance in stacking sequence of the growing material appears as stacking faults. These defects have very small formation energy and according to some theoretical calculations even negative formation energy [14,15]. Thus their appearance is quite common in 3C-SiC.

In our growth experiments 3C-SiC nucleated as two dimensional islands at 1675°C

independently of the substrate face. The initial nucleation was non uniform in case of growth on the Si-face. One could observe area (~1x3 mm^2) with high coverage by 3C-SiC and low TB density, while on the rest of the sample there were just small nuclei. The lowest nuclei density was found in the middle of the sample. The lower nuclei density in the center most probably appears due to a radial temperature gradient. Such one is expected due to the inductive heating of the crucible, which causes higher temperature at the edges and lower in the center of the crucible. In thick (100-250 μm) 3C-SiC layers grown on Si-face we typically observe very similar region (around 2x4 mm^2) having a low density of TBs while in the vicinity of the good region density of TBs was much higher. This was not a single result, as similar regions were also observed earlier when growing 3C-SiC on the Si-face [10]. Thus it seems that on the Si-face the domain was formed at the beginning of growth at a low temperature, when supersaturation ratio was quite low, and with continued growth the primary 3C-SiC island has extended. In other places on the substrate nuclei formed later at higher temperature when supersaturation ratio was higher, thus higher density of nuclei appeared and by expanding they have formed higher density of TBs.

In contrast, at similar conditions the initial nucleation of 3C-SiC on the C-face was much more uniform with small nuclei on the whole growth area. This is attributed to the lower surface free energy of the C-face compared to the Si-face 6H-SiC [12]. The lower surface free energy of the C-face results in a smaller critical supersaturation ratio [16] which is the smallest supersaturation ratio needed for stable nuclei to form. Thus at the same supersaturation ratio higher number of nuclei with more uniform distribution will appear on the C-face compared to Si-face. Additionally, when these nuclei expand and coalesce they form much more uniform TB density over the whole growth area. This is in agreement with our observations in growth experiments on C-face.

The coverage of the 6H-SiC substrate by 3C-SiC on the Si-face was increasing uniformly when the growth temperature was increased from 1675°C to 1775°C. We could observe that on the C-face the 3C-SiC coverage increased when increasing temperature from 1675°C to 1725°C, however coverage did not change further with increasing temperature till 1775°C (table 1). This would mean

that the 3C-SiC coverage on the C-face is determined at the initial growth stage. At later stages it is difficult to overgrow competing 6H-SiC growth centers by an increased layer thickness. This is in fact in agreement with the observation of 6H-SiC spirals in the layers, as discussed below.

Common defects in all samples were triangular features (Fig. 1) which are caused by stacking faults reaching the surface [10]. In contrast to TBs, SFs density on the surface of the grown material was very similar on both faces (~10^2-10^3 cm^{-1}).

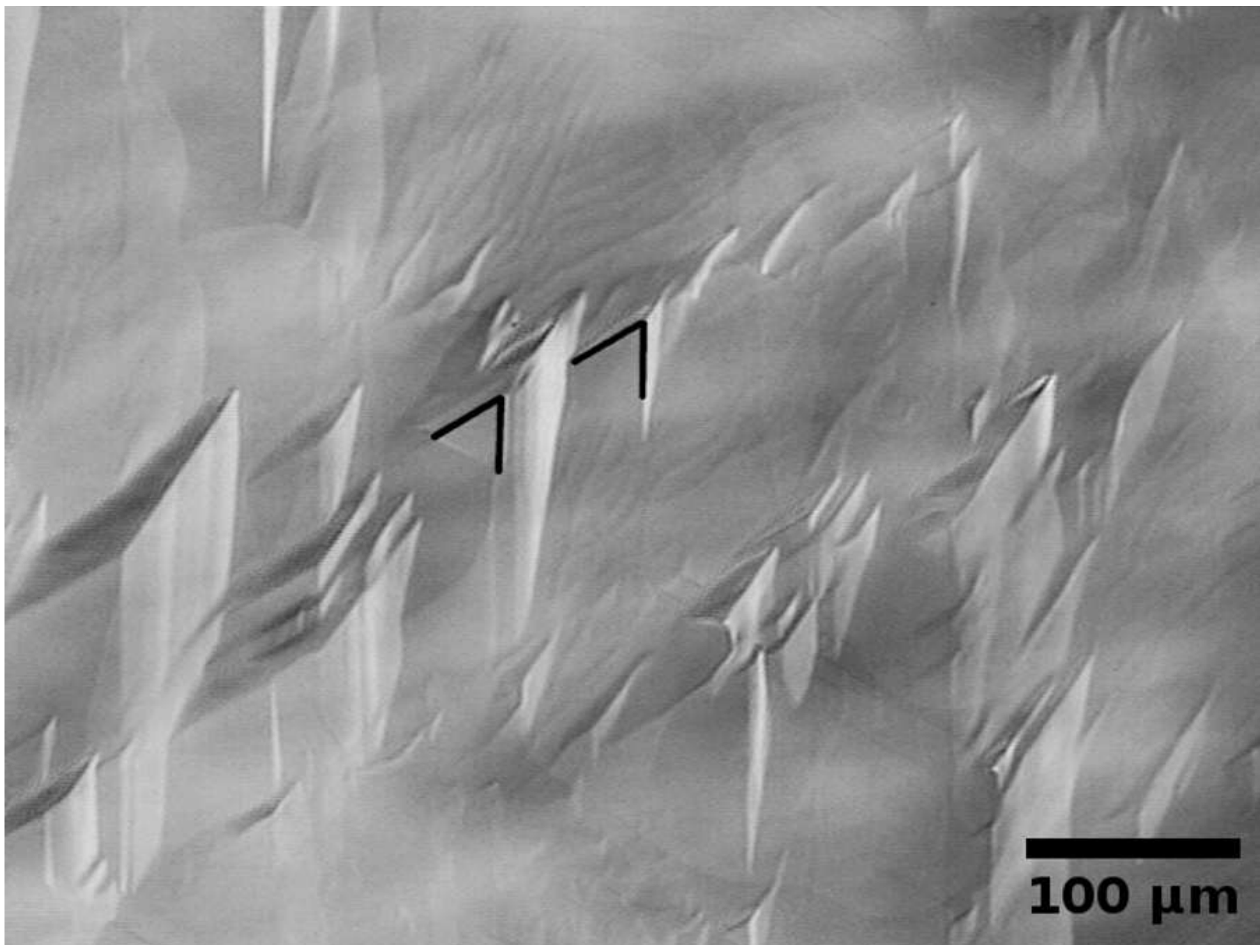

Fig. 1. Typical optical micrograph of stacking faults induced triangular features. The black lines demarcate two of these features.

From the AFM characterization of the 3C-SiC layers we have found that the steps of 0.25 nm height on both faces were dominant. The step terraces were in order of 30-40 nm, which were slightly wider on the Si-face. Additionally, no step bunching was observed in the defect free areas. The step bunching is usually observed when hexagonal SiC polytypes are grown. In that case the smallest step hight of 0.75 or 1.5 nm for 6H-SiC and 0.5 or 1.0 nm for 4H-SiC are observed. The

appearance of step bunching in these polytypes is related to different surface energy of every bilayer, which is not the case for 3C-SiC [17]. However, at the SFs, step flow growth pinning was observed. The pinning disturbs the step flow growth and steps up to 1.5 nm in height were observed. Additionally, surface waviness in order of 5 nm height was observed on both faces, and it was slightly more pronounced on the Si-face.

It was shown earlier [13], that the 3C-SiC nucleation proceeds after homoepitaxial growth of 6H-SiC, by which the quality of subsequently growing 3C-SiC is affected. Thus, it is of importance to also get insight the homoepitaxial growth of 6H-SiC. We have observed that the homoepitaxial 6H-SiC near 3C-SiC regions was growing in spiral mode on both faces. However, the density of 6H-SiC spirals was much higher and their terraces were smaller on the C-face compared to the ones on the Si-face (table 2).

Furthermore, a new type of defects were observed on thick layers of 3C-SiC (>100 μm) grown on the C-face of 6H-SiC substrates. These appear as pits (20-150 μm in diameter) in the 3C-SiC layer with a 6H-SiC spiral on the bottom of the pit (Fig. 2a,b). The depth of the pits depends on the 3C-SiC layer thickness and varies between 0.1-0.3 μm near the edge of the 3C-SiC lateral growth front and up to 1 μm where the 3C-SiC layer was thicker. The density of the pits was very non uniform. It was ~10^5 cm^{-2} near the edge of the 3C-SiC lateral growth front, ~10^3 cm^{-2} where the 3C-SiC layer was 10-50 μm thick and only few pits per square centimeter where the 3C-SiC layer was 100-200 μm thick. The pit density dependence on the layer thickness indicates that they are overgrown by the 3C-SiC. Additionally, there was a higher density of SF at the pits which lowers the layer quality. However, TBs relation with the pits was not observed, meaning that there was no increase or decrease of TBs near the pits or change in the pits density near TBs.

From the AFM analysis of the pits and edges of 3C-SiC domains we propose a model describing the pits formation. The lateral growth of 3C-SiC has to compete with homoepitaxial 6H-SiC growing in the spiral mode. This is illustrated by the OM and AFM in figures 2a and 2b and a schematic image with growth steps is depicted in Fig. 3a. The 3C-SiC growth proceeds in between

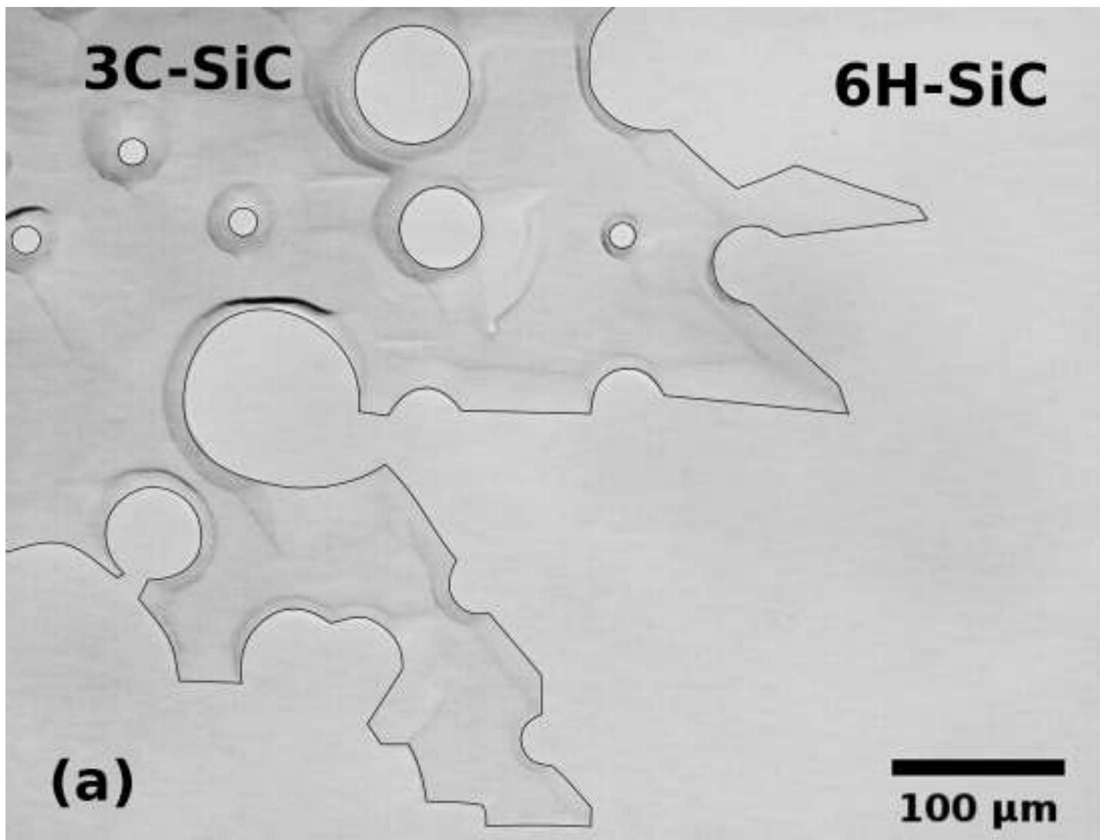

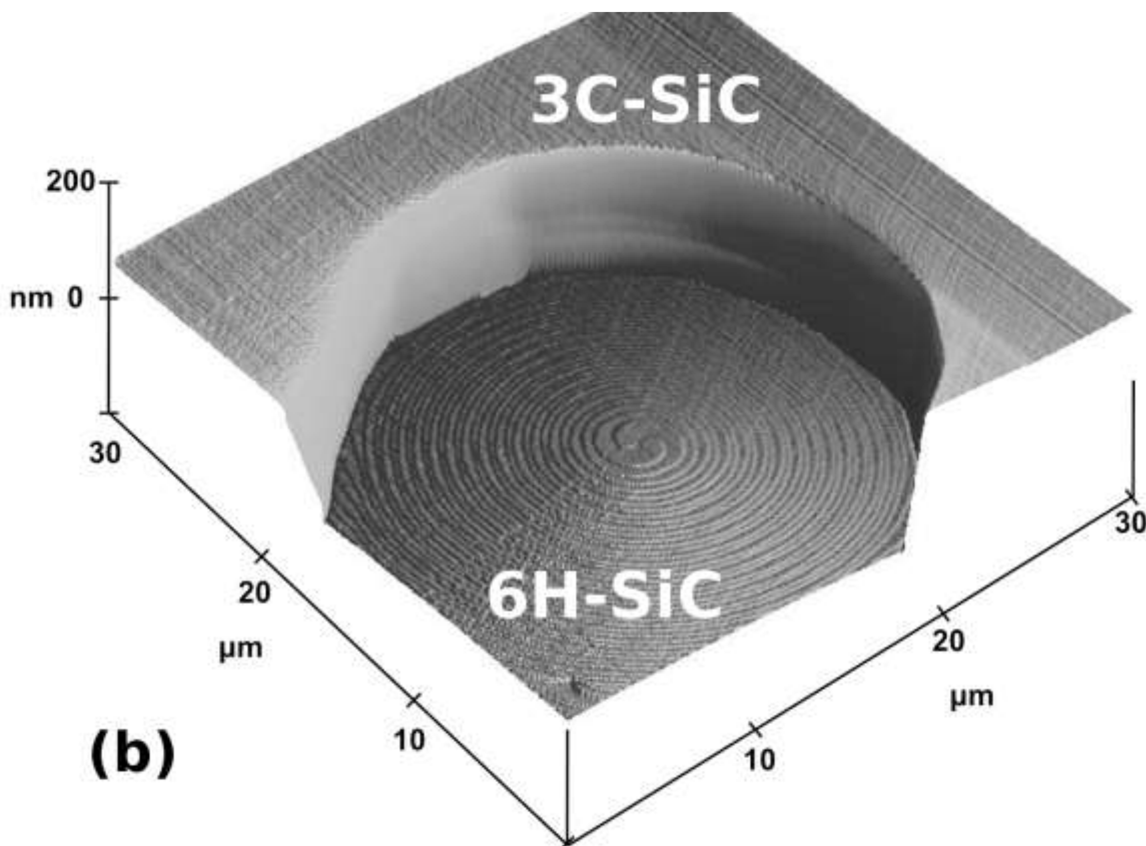

Fig. 2. (a) Optical microscope image of nonuniform lateral growth of 3C-SiC on C-face and formation of pits (roundish features). Contrast between 3C/6H-SiC is artificially increased for easier viewing; (b) AFM image (scan size 30x30 μm) of 6H-SiC spiral growth in a pit (200 nm deep) of 3C-SiC layer.

6H-SiC spirals, where terraces are wider (Fig. 3b) and also the supersaturation ratio is higher [13]. The growth was much slower in the direction where spirals are present. Nevertheless, the normal growth rate in (111) direction of 3C-SiC was higher than that of 6H-SiC growing in spiral mode. Thus, during subsequent growth the 6H-SiC spirals are incorporated in the layer as pits (Fig. 3c) and can be partially or entirely overgrown by 3C-SiC. This is an intriguing finding since spiral growth should be expected to proceed easier than the two dimensional growth for the same material. However in the present case the growth conditions are set for 3C-SiC and apparently this material takes over.

To further elaborate on pits occurrence we have additionally analyzed 3C-SiC layers grown at 1675°C in which we found pits in layers grown on both, Si- and C-faces. However, on layers thicker than 30 μm the pits with 6H-SiC spirals were observed only in the layers grown on the C-face. To understand why the 6H-SiC spirals are overgrown so slowly on the C-face we analyzed the nucleation of 3C-SiC in the frame of the Burton-Cabrera-Frank theory [18,13]. According to [16] nucleation should occur more frequently on the C-face than on the Si-face, if the supersaturation ratio is the same. Thus the 6H-SiC should be overgrown easier on the C-face. However, in our case the result was the opposite. This indicates that probably the supersaturation ratio was different. From [16] we know that the surface diffusion length is higher and as shown in table 2 the terrace widths are smaller on the C-face. These two parameters should influence the supersaturation ratio and subsequently nucleation and growth of 3C-SiC. We have calculated the maximum value of the supersaturation ratio ($\alpha_{max}=n_s/n_{s0}$), which appears in the middle of the step terraces [16,13]:

$$\alpha_{max} = 1 + \frac{\lambda_0 n_0 R}{2\lambda_s h} \frac{\tau_s}{n_{s0}} \tanh\left(\frac{\lambda_0}{4\lambda_s}\right) \qquad (1)$$

where n_s is the number of adsorbed atoms per unit area on the surface, n_{s0} – adatom concentration at equilibrium λ_0 – terrace length, λ_s – surface diffusion length, $n_0 = 1/a^2$ – density of adsorption sites on the surface (1.06 x 10^{15} cm^{-2}), a – lattice constant, R – growth rate, h – step height (0.25 nm),

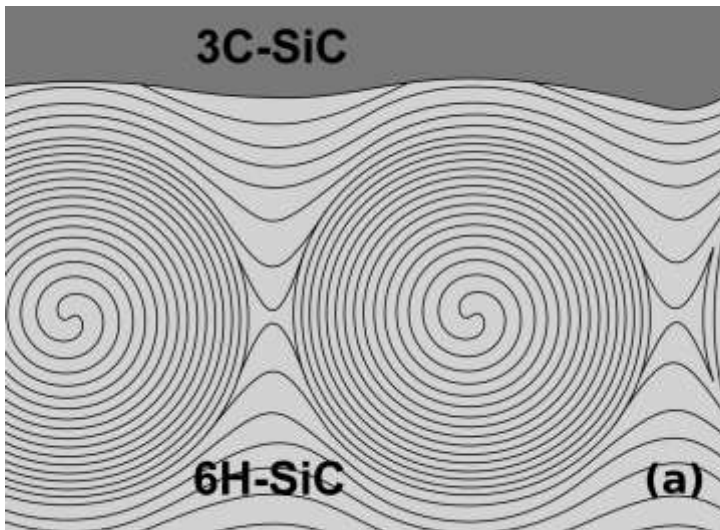

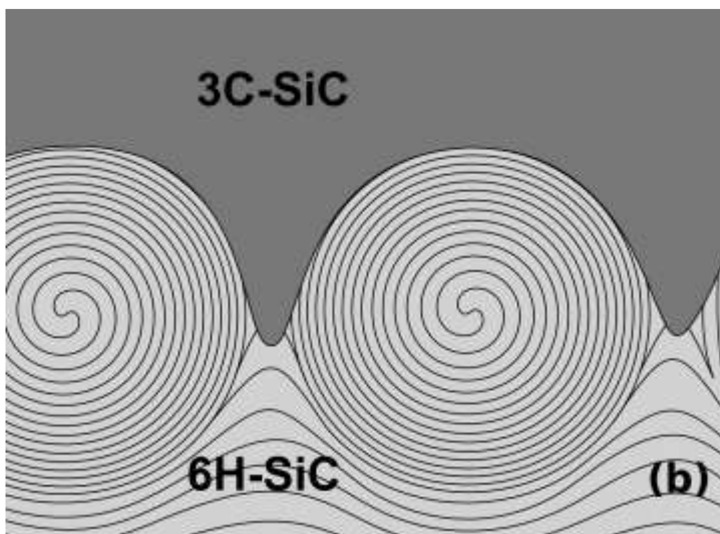

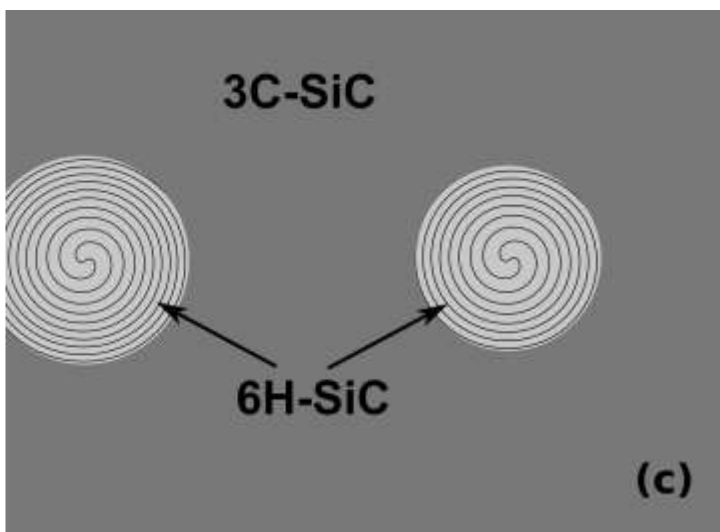

Fig. 3. Lateral growth evolution of 3C-SiC on 6H-SiC substrates. The lines represent step edges.

n_{s0}/τ_s - desorption flux. Surface diffusion length we have taken from [16] and desorption flux from [13]. Terrace length and growth rate are taken from the growth experiments.

Calculated values of maximum supersaturation ratio are shown in table 2. We can see that the supersaturation ratio at 1675°C is higher on the Si-face, compared to the C-face, though the difference is not significant (1.4 times). Seemingly, due to a lower critical supersaturation ratio more nuclei appear and more uniform TB distribution on the C-face has been formed. However, when increasing the temperature to 1775°C the supersaturation ratio increases more than 3 times on the Si-face. This explains the increased 3C-SiC coverage and higher TB density in some areas on the Si-face, when temperature was increased, as the increased maximum supersaturation ratio increases the nucleation rate. At the same time on the C-face the maximum supersaturation ratio has not changed noticeably due to higher surface diffusion length and smaller terraces compared to Si-face. As a consequence, the pits with 6H-SiC spirals could be overgrown very slowly. The big difference in the maximum supersaturation ratio also indicates that the growth of 3C-SiC on the Si-face is much more sensitive to changes in temperature (for example when temperature gradient across the sample is present) compared to the C-face. Thus it may be more difficult to control the growth of 3C-SiC on large area Si-face substrates.

3.2 XRD characterization

To acquire the structural quality of the grown material, XRD ω-rocking curve measurements were conducted. The measurements were performed by scanning the whole sample with a footprint size of 2x2 mm^2 (fig. 4a). The full width at half maximum (FWHM) of the ω-rocking curves for the material grown on the Si-face of 6H-SiC substrate was in the range of 150-500 arcsec over the sample. The best values were measured at the smoothest places with the smallest number of triangular features and TBs. On the other hand, the 3C-SiC layer grown on the C-face 6H-SiC shows FWHM of 550-750 arcsec. The distribution of ω-rocking curves FWHM values over the sample is shown in figure 4b. The higher values are attributed to the higher density of TBs and the

smaller spread of the values is due to more uniform distribution of TBs in 3C-SiC grown on C-face.

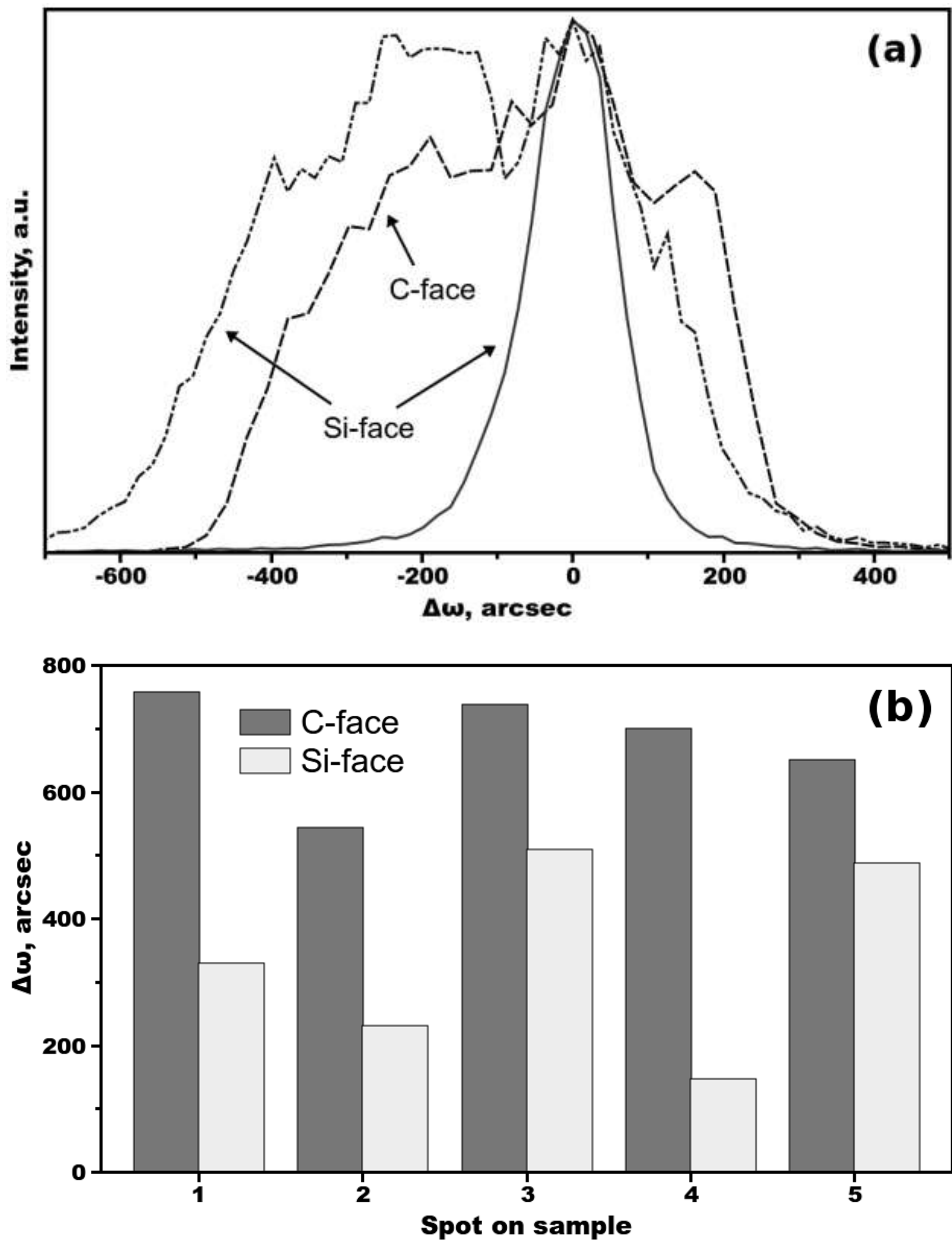

Fig. 4. XRD rocking curve (a) of 3C-SiC grown on Si-face (best and typical) and C-face (typical) of 6H-SiC; (b) scattering of FWHM values over the sample.

In the XRD ω-rocking curves of 3C-SiC grown on C-face one can observe several peaks indicating that the crystal consists of several domains, slightly (50-100 arcsec) tilted to each other. Similar observations have been reported earlier on 3C-SiC epilayers [10]. They were attributed to the misorientation of the 3C-SiC domains, which nucleates as two-dimensional islands and every island can have slightly different orientation. The misorientated domains were observed on both faces. Nevertheless, on the Si-face there were few places (2x4 mm^2) indicating better quality material (FWHM ~150 arcsec) and misorientated domains were not observed in these spots.

3.3 Photoluminescence characterization

Nitrogen (N) and aluminum (Al) are typical background impurities in sublimation grown 3C-SiC material. To evaluate the unintentional doping level of N and Al for different faces the low temperature photoluminescence (LTPL) measurements were carried out. In the LTPL spectra the N bound exciton and also the phonon replicas of 3C–SiC were evident in all samples. A weak peak of the Al bound exciton at ~ 2.365 eV [19] was observed in all samples and very weak Donor Acceptor Pair (DAP) complex was possible to observe in some of the samples indicating that there is no or very small compensation.

The n-type doping concentration was acquired by comparing the full width at half maximum (FWHM) of the TA-phonon replica of the ZPL (zero- phonon line) of the nitrogen bound exciton [20] with the calibration curve from [21]. The Al doping was calculated using a combination of Al bound exciton line intensities with the intensity of the N–Al donor–acceptor pair, if present [10]. The results show that the doping by N was in the range of 10^{16} cm^{-3}, while by Al it was in the 10^{14} cm^{-3} range, with a slight difference depending on the face polarity. Typical results are shown in table 3. The Al doping was higher for the 3C-SiC grown on the Si-face as compared to the C-face, while N doping was slightly lower on the Si-face. These tendencies of face dependent doping are similar to the ones for hexagonal SiC polytypes (4H and 6H-SiC) [22]. This result shows that the difference in doping depends only on the face polarity, but not on the polytype.

It is interesting to note, that generally LTPL intensities for the 3C-SiC grown on C-face were higher, indicating lower non-radiative recombination even though structural quality seems worse.

4. Conclusions

The 3C-SiC (111) growth proceeds differently on Si- and C-faces of nominally on-axis 6H-SiC substrates by sublimation growth technique, although no significant difference in the overall growth rate was observed between the two faces.

Due to energetic reasons C-face provides more favorable conditions for uniform nucleation in comparison with the Si-face. New type of defects, that is, pits, was observed in the material grown on the C-face. Pits are related to spiral growth of the homoepitaxial 6H-SiC layer preceding the 3C-SiC formation. It was shown that the maximum supersaturation ratio was similar on both faces at a temperature of 1675°C. After an increase of the temperature to 1775°C the maximum supersaturation ratio increased more than 3 times on the Si-face, however, on the C-face it was almost the same as at the previous temperature. Thus most of the 6H-SiC spirals were overgrown by 3C-SiC on the Si-face, but not on the C-face, where they are incorporated as pits.

The FWHM values of ω-rocking curves were larger (550-700 arcsec) on the C-face grown material, but the spread of the values was smaller. This can be explained by more uniform nucleation.

Unintentional Al doping was lower and N doping slightly higher on the C-face grown 3C-SiC, which follows the same pattern as for hexagonal SiC polytypes. On the grown 3C-SiC layers no step bunching was observed on both faces of 3C-SiC in defect free areas. This is an advantage for growth of graphene on 3C-SiC and should improve its quality compared to graphene on 6H-SiC.

Acknowledgments

The work was supported by the Swedish Research Council (VR contract 2008-5753), Ångpanneföreningens Forskningsstiftelse and Ericsson’s Research Foundation. Authors

acknowledge R. Liljedahl for the help with XRD measurements. M. Syväjärvi acknowledges Swedish Energy Agency.

References

[1] M. Suemitsu, Y. Miyamoto, H. Handa, A. Konno, J. Surf. Sci. Nanotech. 7 (2009) 311-313.

[2] A. Luque, A. Marti, Phys. Rev. Lett. 78 (1997) 5014-5017.

[3] J.A. Powell, J.B. Petit, J.H. Edgar, I.G. Jenkins, L.G. Matus, J.W. Yang, P. Pirouz, W.J. Choyke, L. Clemen, M. Yoganathan, Appl. Phys. Lett. 59 (1991) 333-335.

[4] F.R. Chien, S.R. Nutt, W.S. Yoo, T. Kimoto, H. Matsunami, J. Cryst. Growth 137 (1994) 175-180.

[5] P.G. Neudeck, A.J. Trunek, D.J. Spry, J.A. Powell, H. Du, M. Skowronski, X.R. Huang, M. Dudley, Chem. Vapor Depos. 12 (2006) 531-540.

[6] A.A. Lebedev, Semicond. Sci. Technol. 21 (2006) R17–R34.

[7] H.S. Kong, J.T. Glass, R.F. Davis, J. Mater. Research 4, (1989) 204-214.

[8] L. Latu-Romain, D. Chaussende, P. Chaudouet, F. Robaut, G. Berthome, M. Pons, R. Madar, J. Cryst. Growth 275 (2005) e609–e613.

[9] O. Kim-Hak, G. Ferro, J. Dazord, M. Marinova, J. Lorenzzi, E. Polychroniadis, P. Chaudouet, D. Chaussende, P. Miele, J. Cryst. Growth 311 (2009) 2385–2390.

[10] R. Vasiliauskas, M. Marinova, M. Syväjärvi, R. Liljedahl, G. Zoulis, J. Lorenzzi, G. Ferro, S. Juillaguet, J. Camassel, E.K. Polychroniadis, R. Yakimova, J. Cryst. Growth 324 (2011) 7-14.

[11]M. Sabisch, P. Kruger, J. Pollmann, Phys. Rev. B 55 (1997) 10561-10570.

[12] R. Yakimova, M. Syväjärvi, E. Janzen, Mat. Sci. Forum 264-268 (1998) 159-162.

[13] R. Vasiliauskas, M. Marinova, P. Hens, P. Wellmann, M.Syväjärvi, R. Yakimova, Cryst. Growth Des. 12 (2012) 197−204.

[14] P. Käckell, J. Furthmüller, F. Bechstedt, Phys. Rev. B 58 (1998) 1326-1330.

[15] H. Iwata, U. Lindefelt, S. Oberg, P.R. Briddon, J. Phys.: Condens. Matter 14 (2002) 12733–

12740.

[16] T. Kimoto, H. Matsunami, J. Appl. Phys. 75 (1994) 850-859.

[17] T. Kimoto, A. Itoh, H. Matsunami, T. Okano, J. Appl. Phys. 81 (1997) 3494-3500.

[18] J.P. Hirth, G.M. Pound, Condensation and Evaporation: Nucleation and Growth Kinetics; Pergamon, Oxford, 1963, Chaper B.

[19] L.L. Clemen, R.P. Devaty, M.F. MacMillan, M. Yoganathan, W.J. Choyke, D.J. Larkin, J.A. Powel, J.A. Edmond, H.S. Kong, Appl. Phys. Lett. 62 (1993) 2953.

[20] W.J. Choyke, D.R. Hamilton, L. Patrick, Phys. Rev. 133 (1964) A1163.

[21] J. Camassel, S. Juillaguet, M. Zielinski, C. Balloud, Chem. Vapor Dep. 12 (2006) 549.

[22] T. Kimoto, A. Itoh, H. Matsunami, Appl. Phys. Lett. 67 (1995) 2385-2387.

Tables:

Table 1. Substrate coverage by 3C-SiC at different growth temperatures.

Temperature (°C)	Si-face (%)	C-face (%)
1675	10-20	10-20
1725	40-50	80-85
1775	85-90	85-90

Table 2. Surface features and maximum supersaturation ratio for homoepitaxial 6H-SiC.

	Si-face	C-face
Step height (nm)	1.5	0.75
Terrace width (nm) at 1675 °C	400-650	350-500
Terrace width (nm) at 1775 °C	600-800	200-300

Spiral density (cm^{-2})	~10^3	~10^5
α_{max} at 1675 ^{o}C	1.45	1.002
α_{max} at 1775 ^{o}C	4.49	1.004

Table 3. Residual doping of the 3C-SiC, as acquired from LTPL measurements.

Dopant	Si-face	C-face
N (cm^{-3})	3.7x10^{16}	4x10^{16}
Al (cm^{-3})	8x10^{14}	2x10^{14}